23rd ABCM International Congress of Mechanical Engineering
December 6-11, 2015, Rio de Janeiro, RJ, Brazil

MODELING, PARAMENTER ESTIMATION AND STATE-SPACE CONTROL OF A STEAM TURBINE

Rodrigo Trentini
Rüdiger Kutzner
Faculty I - Electrical Engineering and Information Technology – University of Applied Sciences and Arts Hannover, Ricklinger Stadtweg 120, 30459, Hannover, Germany
rodrigo.trentini@hs-hannover.de
ruediger.kutzner@hs-hannover.de

Lutz Hofmann
Institute of Electric Power Systems, Division of Power Supply – University of Hannover, Appelstraße 9a, 30167, Hannover, Germany
hofmann@iee.uni-hannover.de

Alexandre Campos
Superior Educational Center of Itajaí's Mouth – Santa Catarina State University, Avenida Central 413, 88330-668, Balneário Camboriú, Brazil
alexandre.campos@udesc.br

Clodoaldo Schutel Furtado Neto
Center of Technological Sciences – Santa Catarina State University, Rua Paulo Malschitzki 200, 89219-710, Joinville, Brazil
clo_neto@msn.com

Abstract. *This paper presents an innovative approach for modeling a steam turbine which is fully based on the Mass and Energy Conservation Principle from Fluid Mechanics. The main difference between literature stands for the consideration of turbine's High, Intermediate and Low Pressure sections as resistive pipes, which simplifies considerably system's equating. The system is then linearized to a 6^{th}-order one aiming its identification and control. Turbine's internal parameter determination is addressed by the so-called Particle Swarm Optimization method, ensuring system's state space structure after identification. The identification results show that the proposed model is able to depict the current modeling with more than 96% of accuracy. Further, using state information from an optimum state observer (Kalman Filter) torque and frequency are regulated through the feedback of system's states also using an optimal approach (Linear Quadratic Regulator), where is shown that using a controller which accounts for the noise, control signal's variance is 5.5 times smaller than with an ordinary Proportional-Integral one.*

Keywords: *Modeling of Steam Turbine, Particle Swarm Optimization, Optimum Control.*

1. INTRODUCTION

According to the *Law of Parsimony*, among competing hypotheses that represent equally well a system, the simplest one should be selected. More complex solutions may provide either better predictions or other possibilities for the same prediction. In other words, one must consider always the trade-off between complexity and accuracy. This principle is be kept in mind during the development of the present work.

It is widely known in Power Systems Stability field that steam turbine's sections can be represented as first-order systems (Grigsby, 2012). It reduces dramatically the difficulty of its analysis and implementation, since considering all Fluid Mechanics laws to describe its behavior would increase indefinitely system's model. Furthermore this simple modeling depicts with enough accuracy – for this specific aim – the dynamics of turbine's torque (Kundur *et al.*, 1994).

Indeed there are many researches which deal with detailed turbine models aiming simulation. Chaibakhsh and Ghaffari (2008) developed a nonlinear model where turbine's sections are based on the energy balance, thermodynamic state conversion and semi-empirical equations. Then, the related parameters are either determined by empirical relations obtained from experimental data or they are adjusted by applying genetic algorithms. The final model provides access to turbine's internal states and it is accurate enough for simulation purposes, with accuracy up to 0.3%, however it is not suitable for control design due to its complexity. Jiang *et al.* (2010) introduce a new model focused on the nonlinearities between flow rate and pressure change, besides reflecting enthalpy variations on the dynamic responses. The simulation results based on the identified model show reasonable agreement according to the test data. Zimmer (2008) presents an interesting work where three different models are analyzed: a linear and a simplified and other accurate nonlinear ones, where the latter incorporates mass and energy balance as well as the major turbine's nonlinearities.

The main issue is that this increase in system's complexity does not present strong benefits which justifies its use in Power Systems Stability analysis, since power systems models are intrinsically complex themselves.

However, looking at controller's side, the lack of information on turbine's internal states limits its design to the classic control approach. Undoubtedly the access to internal states opens many other possibilities on controlling dynamic systems, such as optimum control (Ogata, 1970). It leads immediately to a control-based steam turbine model where its internal states can be directly measured or at least observed.

Another issue to be addressed is that a complete mathematical model of the steam turbine does not ensure the designer that all internal parameters are known. In fact some of them are hard to determine if not provided by the manufacturer, which is seldom the case for currently implemented turbines. Without knowing turbine's internal parameters is not possible to determine its internal states. Fortunately in this case the matter can be addressed by using System Identification techniques. Nevertheless ordinary Least Squares is not an option since it gives results for polynomial models and in this work we intend to stick on state space models due to the reasons cited before.

Hence, this paper intends to develop an innovative equating for the steam turbine where the access to its internal states is available. It will be shown through the paper that it is possible to reach results similar to the ones obtained using common turbine model, but in state space approach, therefore achieving the previous cited trade-off between complexity and accuracy. To reach this goal it is necessary to perform parameter estimation, which is addressed through the so-called Particle Swarm Optimization (PSO) algorithm. From these results the Linear Quadratic Gaussian (LQG) controller is designed and compared to an ordinary Proportional-Integral (PI) one.

The paper is organized as follows: Section 2 addresses the current and proposed modeling of steam turbine, including its linearization. Section 3 tackles the parameter estimation of both proposed models using PSO, besides its evaluation using current turbine model as basis. Section 4 shows PI's and LQG's controller design, whereas its results are presented in Sec. 5. In Sec. 6 the conclusions and next steps for this research are presented.

2. MODELING

Several distinct steam turbines types are currently available depending mainly on size and steam conditions. In this work a *single-reheat tandem-compound* steam turbine will be studied. Figure 1 depicts its main components aiming modeling.

Turbine's accumulators are named in this paper as *vessels*, namely *Chest*, *Reheater* – where the steam is heated up again – and *Crossover*. The places where steam produces work are called *sections*, namely *High-Pressure (HP)*, *Intermediate-Pressure (IP)* and *Low-Pressure (LP)*. Each section consists of moving and stationary blazes which ensure gas speed, *i.e.* mass flow rate, to be unchanged after leaving it. Control valve is represented in Fig. 1 as *CV*, which is properly system's actuator, and where the controller signal is applied. Turbine's mechanical torque τ_M is system's output. Condenser and intercept valve are neglected in this work. For more details on steam turbines working principle, please refer to Kundur *et al.* (1994).

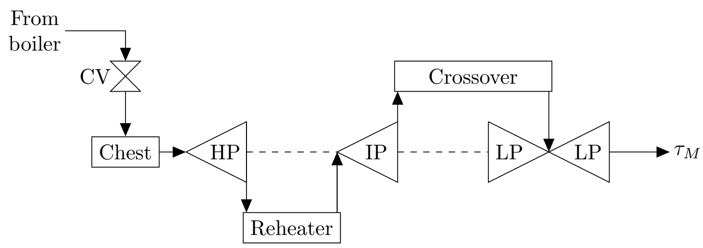

Figure 1: Common configuration of single-reheat tandem-compound steam turbine (based on Kundur *et al.* (1994))

Next sections will present steam turbine common equating – named here *current modeling* – and the proposed model. Both are developed through Mass and Energy Conservation Principle from Fluid Mechanics and their main difference, as previously stated, is the access to turbine's internal states.

2.1 Current Modeling

The purpose of this section is to demonstrate the origin of the most used steam turbine's model whenever Power System Stability analysis is aimed, since just few information on its modeling is available in the main literature on this theme (see *e.g.* Grainger and Stevenson (1994), Eremia and Shahidehpour (2013) and Grigsby (2012)), intending for a comparison between the presented (from now on just *simplified model*) and the proposed models.

To reach the proposed final end for this section, the following assumptions must be considered:

- the mixture of steam and dry gas can be considered as an ideal gas;
- the vessel has constant volume and temperature, *i.e.* $\dot{V} = \dot{T} = 0$;
- the total amount of mass in the vessel is equal to the difference between what enters and what leaves it, *i.e.* $m = m_{in} - m_{out}$;
- the heights of inlet and outlet orifices are the same, *i.e.* $z_1 = z_2$;
- the areas of inlet and outlet orifices are the same, *i.e.* $A_1 = A_2$.

Starting from the time derivative of the Ideal Gas Law for one pressure vessel:

$$\dot{m}_{in} - \dot{m}_{out} = \frac{V}{RT}\dot{P}, \tag{1}$$

where $\dot{m}_{in}$ and $\dot{m}_{out}$ are the entering and leaving mass flow rates, R is the specific gas constant and P is the pressure inside the vessel. Taken into account the density as $\rho = \frac{m}{V}$, one finds that $\frac{\partial\rho}{\partial P} = \frac{1}{RT}$, and thus,

$$\dot{m}_{in} - \dot{m}_{out} = V\dot{\rho}. \tag{2}$$

Considering the previous simplifications (and also $P_1 = P_o =$ cte, $P_2 = P$ and $\dot{m}_{in} =$ cte), the time derivative of Bernoulli's equation results in,

$$\dot{P} = \frac{P_o}{\dot{m}_{in}}\ddot{m}_{out}, \tag{3}$$

with P_o being the rated pressure. Substituting Eq. 3 in Eq. 2,

$$\ddot{m}_{out} = \frac{RT}{VP_o}\dot{m}_{in}\dot{m}_{out} + \frac{RT}{VP_o}\dot{m}_{in}^2, \tag{4}$$

which is clearly a nonlinear equation. The equilibrium condition is obtained with $\ddot{m}_{out} = 0$, resulting in $\bar{\dot{m}}_{out} = \bar{\dot{m}}_{in} = \dot{m}_o$, with $\dot{m}_o$ being the rated mass flow rate out of the vessel. Applying Taylor's series and truncating it in the first term, one obtains,

$$\ddot{m}_{out} \approx \frac{RT}{VP_o}\dot{m}_o\left(\dot{m}_{in} - \dot{m}_{out}\right). \tag{5}$$

Considering $\mathrm{T} = \frac{VP_o}{RT\dot{m}_o}$ and converting Eq. 5 to Laplace's complex domain it results in:

$$\boxed{\frac{\dot{M}_{out}}{\dot{M}_{in}} = \frac{1}{\mathrm{T}s+1},} \tag{6}$$

which is the simplified expression for the mass flow rate evolution into each of turbine's accumulators, namely *Chest*, *Reheater* and *Crossover*. Figure 2 shows the schematic of the simplified turbine, where one identifies the cited accumulators with their time constants T_{ch}, T_{re} and T_{cr}, the main steam pressure from the boiler P_{in}, the fractions of total power generated by turbine's sections k_{hp}, k_{ip} and k_{lp}, and its torque output τ_M.

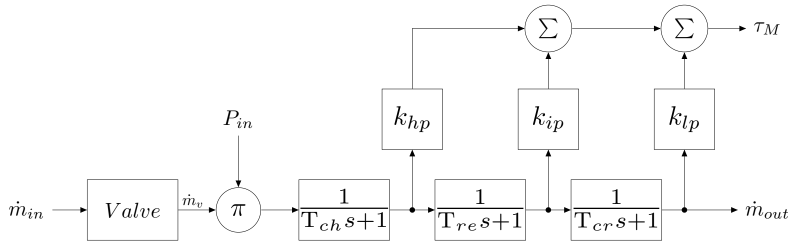

Figure 2: Generic model for a simplified steam turbine (based on Kundur *et al.* (1994))

2.2 Proposed Modeling

Last section has shown that it is possible to represent the behavior of a steam turbine considering each vessel as a first-order system, along with a gain which represents each turbine section.

The actual section expands the just shown equating in order to access the internal states of the machine, namely pressure and temperature of each turbine part. The main aim is to obtain a complete simulation model and afterwards perform its linearization aiming the controller design. Since the proposed model is meant to be more complex than the simplified one, new assumptions must be taken into account. They are:

- pressure P, temperature T and specific mass ρ are uniform into the chambers;
- kinetic and gravitational energies are negligible, as well as the viscous work of the fluid;
- the mixture of steam and dry gas can be considered as an ideal gas;
- the vessel has constant volume, *i.e.* $\dot{V} = 0$;
- the total amount of mass in the vessel is equal to the difference between what enters and what leaves it, *i.e.* $m = m_{in} - m_{out}$;
- the whole system is free from leakages.

With this said, the following sections will deal with vessel's and section's dynamics, besides system's linearization.

2.2.1 Vessel's dynamics

Temperature evolution: The internal energy balance inside a pressure vessel is obtained through the First Law of Thermodynamics, *i.e.* the total transferred energy to a system is equal to the variation of its internal energy:

$$dU + dE_c + dE_p = \delta W + \delta Q, \tag{7}$$

with dU being the variation of the internal energy, dE_c the variation of kinetic energy, dE_p the variation of potential energy, δW the work of external forces and δQ the heat transfer with the ambient. These variables are depicted as (Brun, 1999):

$$\begin{aligned}
dU &= \left[(m + dm_{in})\, c_v \,(T + dT) + dm_{out} c_v T_{out} \right] - \left[(m + dm_{out})\, c_v \,(T + dT) + dm_{in} c_v T_{in} \right], && (8)\\
&= m c_v dT + dm_{in} c_v \,(T - T_{in}) + dm_{out} c_v \,(T_{out} - T)^{1}, && (9)\\
dE_c &= dm_{out} \frac{v_{out}^2}{2} - dm_{in} \frac{v_{in}^2}{2}, && (10)\\
dE_p &= 0, && (11)\\
\delta W &= \frac{P_{in}}{\rho_{in}} dm_{in} - \frac{P_{out}}{\rho_{out}} dm_{out}, && (12)
\end{aligned}$$

where T is the gas temperature, v is the gas speed and c_v is the specific heat at constant volume. The sub-indices in and out stand for the amount of entering and exiting gas, respectively.

Thus, combining equations 8-12 with Eq. 7 one finds the internal energy balance, which is given by:

$$m c_v dT + c_v T (dm_{in} - dm_{out}) = dm_{in} \left(c_v T_{in} + \frac{p_{in}}{\rho_{in}} + \frac{v_{in}^2}{2} \right) - dm_{out} \left(c_v T_{out} + \frac{p_{out}}{\rho_{out}} + \frac{v_{out}^2}{2} \right) + \delta Q \tag{13}$$

From Eq. 13 it is possible to notice that $m c_v dT = U$, $dW = 0$ and $dm = dm_{in} - dm_{out}$. So, with h being system's enthalpy, the First Law of Thermodynamics for open systems becomes,

$$\dot{U} = h_{in} \dot{m}_{in} - h_{out} \dot{m}_{out} + \dot{Q}. \tag{14}$$

Then, taking into account equations 13 and 14 one obtains:

$$m c_v \dot{T} = \dot{m}_{in} \left(c_v T_{in} + \frac{p_{in}}{\rho_{in}} + \frac{v_{in}^2}{2} \right) - \dot{m}_{out} \left(c_v T_{out} + \frac{p_{out}}{\rho_{out}} + \frac{v_{out}^2}{2} \right) + \dot{Q}. \tag{15}$$

Now, from the previous hypothesis one can write:

$$\begin{aligned}
&c_v T + \tfrac{P}{\rho} = c_p T = h, && h + \tfrac{v^2}{2} = \text{cte}, && c_p T_{in} + \tfrac{v_{in}^2}{2} = c_p T_u,\\
&c_p T_{out} + \tfrac{v_{out}^2}{2} = c_p T, && \tfrac{c_p}{c_v} = \gamma, && c_v = \tfrac{R}{\gamma - 1},
\end{aligned}$$

with T_u being the upstream temperature of the fluid considering an infinite tank so that the flow velocity is zero and γ the ratio between constant pressure and constant volume specific heats.

Finally, after some algebraic manipulations one obtains the equation for the temperature evolution inside a pressure vessel:

$$\boxed{\dot{T} = (\gamma T_u - T) \frac{RT}{PV} \dot{m}_{in} - (\gamma - 1) \frac{RT^2}{PV} \dot{m}_{out} + (\gamma - 1) \frac{T}{PV} \dot{Q}}. \tag{16}$$

[1] Equation 9 is obtained neglecting the high order terms of Eq. 8.

Pressure evolution: The pressure evolution inside a vessel is given directly by the time derivative of the Ideal Gas Law:

$$\dot{P} = \frac{RT}{V}(\dot{m}_{in} - \dot{m}_{out}) + \frac{P}{T}\dot{T}. \tag{17}$$

Therefore, substituting Eq. 16 into Eq. 17 one obtains the final expression for it:

$$\boxed{\dot{P} = \frac{\gamma R T_u}{V}\dot{m}_{in} - \frac{\gamma R T}{V}\dot{m}_{out} + \frac{(\gamma - 1)}{V}\dot{Q}}. \tag{18}$$

Heat transfer: The heat transfer is given directly by Newton's Cooling Law:

$$\boxed{\dot{Q} = -\lambda(P,T)A_q(T - T_a)} \tag{19}$$

being $\lambda(P,T)$ the coefficient of convective heat transfer between the gas and the wall (heat transfer by radiation and thermal capacity of the vessel walls are neglected), A_q is the surface area of the vessel and T_a is the ambient temperature.

According to Carneiro and Almeida (2006), $\lambda(P,T)$ can be given by,

$$\lambda(P,T) = \lambda_o \left(\frac{PT}{P_o T_o}\right)^{0.5}, \tag{20}$$

where λ_0 and T_0 are the heat transfer coefficient and the temperature at equilibrium conditions, respectively.

It is important to highlight that Eq. 19 considers the heat transfer between vessel's walls and the environment. The heat transfer between the gas inside the vessel and vessel's walls is not considered, *i.e.* the walls are meant to be at the same temperature as the gas inside it.

Mass flow rate: The mass flow rate for turbine's inlet and outlet orifices is modeled as a flow through a convergent nozzle. In this case, two further assumptions must be taken into account: there is no friction in the system and the flow is reversible and adiabatic, *i.e.* there is no heat transfer during the flow. The latter can be considered a good approach because the flow is usually fast so that the heat transfer can be neglected (Fox and McDonald, 2008).

In such approach there are two different behaviors for the mass flow rate:

$$\boxed{\dot{m} = \begin{cases} P_u A \sqrt{\frac{2\gamma}{RT_u(\gamma-1)}\left[\left(\frac{P_d}{P_u}\right)^{\frac{2}{\gamma}} - \left(\frac{P_d}{P_u}\right)^{\frac{\gamma+1}{\gamma}}\right]} & \text{for subsonic flow,} \\ P_u A \sqrt{\frac{\gamma}{RT_u}\left(\frac{2}{\gamma+1}\right)^{\frac{\gamma+1}{\gamma-1}}} & \text{for sonic flow,} \end{cases}} \tag{21}$$

being P_u and T_u the upstream pressure and temperature respectively, P_d the downstream pressure and A the effective area of flow.

2.2.2 Section's dynamics

So far the presented steam turbine model does not differentiate from any ordinary equating for pressure vessels (see *e.g.* Ali *et al.* (2009), Blagojević and Stojiljković (2007) and Bobrow and McDonell (1998)). However, modeling of turbine's sections is still an issue to be addressed, as stated in Section 1. The present section shows an approach to simplify pressure, temperature and mass flow rate into each turbine section.

Temperature evolution: According to Carneiro and Almeida (2006), the temperature dynamics is often simplified in literature by accounting for the following polytropic law:

$$\boxed{T_{out} = T_{in}\left(\frac{P_{out}}{P_{in}}\right)^{\frac{\gamma-1}{\gamma}}}, \tag{22}$$

which is considered in this work for temperature evolution into each turbine section.

Pressure evolution: It is known that inside a turbine section the gas speed increases and decreases when it passes through the fixed and moving blazes respectively, maintaining, at section's outlet, its velocity unchanged with regarding to the input one.

Therefore it is possible to consider *HP*, *IP* and *LP* sections as pipes, where the gas speed, and consequently the mass flow rate, is constant and there is a drop in pressure and temperature along the pipe due to friction of the gas with pipe's walls.

Using Darcy-Weisbach Equation, the pressure evolution at section's outlet can be represented as:

$$\boxed{P_{out} = P_{in} - \frac{k_f(\dot{m})T_{in}\dot{m}}{P_{in}}}, \tag{23}$$

where $k_f(\dot{m})$ is section's friction coefficient. It depends, in principle, on the geometry of the section and on the Reynolds number, *i.e.* the type of flow regime inside the section.

Mass flow rate: Since the exiting mass flow rate must be the same as the entering one due to turbine's characteristics, a possible approach is to consider just a time delay between input and output:

$$\boxed{\ddot{m}_{out} = \frac{1}{\mathrm{T}_s}\left(\dot{m}_{out} - \dot{m}_{in}\right)}, \tag{24}$$

with T_s being the time constant of the section. Richer and Hurmuzlu (2000) shows that this time delay can be represented as $\mathrm{T}_s = \frac{L_s}{c}$, where L_s is the length of the section and c is the speed of sound in the considered gas.

Finally, using equations 16, 18, 19 and 21 for the vessels (*i.e.*, *Chest*, *Reheater* and *Crossover*), and equations 22, 23 and 24 for the sections (*i.e HP*, *IP* and *LP*), the proposed model is fully described. Figure 3 shows its block diagram.

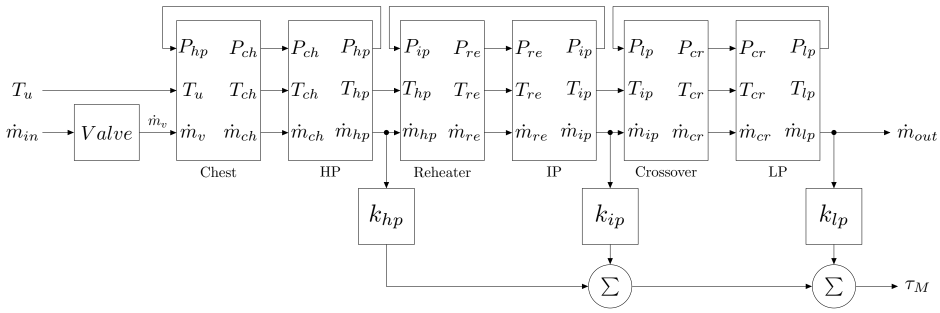

Figure 3: Proposed model for the steam turbine

2.2.3 Linearization

Despite of describing some internal states of the steam turbine, the model presented so far is not suitable for control and parameter estimation purposes due to its strong nonlinear characteristics. Therefore, the linearization of the proposed model is carried out in this section.

However, before applying Taylor's series directly in model's equations, further simplifications can be done:

- T_s is much lower than turbine's time constant, so that from Eq. 24 $\dot{m}_{out} = \dot{m}_{in}$;
- the *Chest* and *Crossover* vessels do not change heat with the ambient, *i.e.* $\dot{Q}_{ch} = \dot{Q}_{cr} = 0$;
- the ambient temperature T_a is constant.

The equilibrium points are obtained doing $\dot{T}_{ch} = \dot{T}_{re} = \dot{T}_{cr} = \dot{P}_{ch} = \dot{P}_{re} = \dot{P}_{cr} = \dot{Q}_{re} = 0$. Now, using equations 16, 18, 19, 21, 22 and 23, applying Taylor's series and truncating it in the first term, one obtains the linearized model for the proposed steam turbine:

$$\begin{aligned}
\begin{bmatrix} \Delta\dot{P}_{ch} \\ \Delta\dot{T}_{ch} \\ \Delta\dot{P}_{re} \\ \Delta\dot{T}_{re} \\ \Delta\dot{P}_{cr} \\ \Delta\dot{T}_{cr} \end{bmatrix} &\approx \begin{bmatrix} K_1 & K_2 & 0 & 0 & 0 & 0 \\ K_4 & K_5 & 0 & 0 & 0 & 0 \\ K_7 & K_8 & K_9 & K_{10} & 0 & 0 \\ K_{11} & K_{12} & K_{13} & K_{14} & 0 & 0 \\ 0 & 0 & K_{15} & K_{16} & K_{17} & K_{18} \\ 0 & 0 & K_{19} & K_{20} & K_{21} & K_{22} \end{bmatrix} \begin{bmatrix} \Delta P_{ch} \\ \Delta T_{ch} \\ \Delta P_{re} \\ \Delta T_{re} \\ \Delta P_{cr} \\ \Delta T_{cr} \end{bmatrix} + \begin{bmatrix} K_3 \\ K_6 \\ 0 \\ 0 \\ 0 \\ 0 \end{bmatrix} \Delta\dot{m}_{in}, \\
\Delta\tau_M &\approx \begin{bmatrix} K_{23} & K_{24} & K_{25} & K_{26} & K_{27} & K_{28} \end{bmatrix} \begin{bmatrix} \Delta P_{ch} & \Delta T_{ch} & \Delta P_{re} & \Delta T_{re} & \Delta P_{cr} & \Delta T_{cr} \end{bmatrix}^T.
\end{aligned} \tag{25}$$

For the sake of readability turbine's internal parameters described in the previous sections are grouped into constants K_1-K_{28}. Next section presents an approach for determining these parameters using simulated data from the model depicted in Fig. 3.

3. PARAMETER IDENTIFICATION

Perhaps the most difficult point to support the equating presented so far is the lack of internal parameters knowledge of the model developed in Sec. 2.2. In fact, some internal quantities of each vessel/section such as heat transfer (λ_0) and friction (k_f) coefficients are difficult to determine without empirical experiments. Others such as the areas of flow (A), the surface areas of the vessels (A_q) and the volumes (V) needed to be measured, which is not possible in many practical cases. Without knowing the cited constants it is not possible to determine coefficients K_1-K_{28} presented in Sec. 2.2.3.

Therefore, in order to establish a feasible model for simulation and posterior control, this section deals with the identification of model's unknown constants. The chosen method for performing identification is the so-called Particle Swarm Optimization, from now on just PSO, discussed in more details in next section. Parameters of the nonlinear model are determined from the parameter estimation of the linerized one (Eq. 25) through a simple comparison which is presented in Section 3.2. At last the evaluation of the proposed model is addressed in order to check its accuracy when compared to the traditional one shown in Fig. 2.

However, before proceeding with the identification it is required to define which signals will be used for this end. As stated in Sec. 1, despite of being a very simplified model, the steam turbine represented in Fig. 2 is able to depict turbine's output torque τ_M with enough accuracy whenever its operation is concerned within a small range (around $\pm$ 5% of its rated operating point) (Kundur *et al.*, 1994).

Therefore, since the cited simplified model is often used by many researchers aiming power systems stability analysis, and due to the lack of experimental values from a real steam turbine, this work considers the simulated output torque τ_M obtained from the model shown in Fig. 2. The input signal $\dot{m}_v$ is randomly defined in order to experiment several possible levels and response times from the system. Figure 4 shows the obtained torque for the cited input profile using the simplified turbine model according to the parameter data shown in Tab. 1. Using these data the PSO algorithm is initialized.

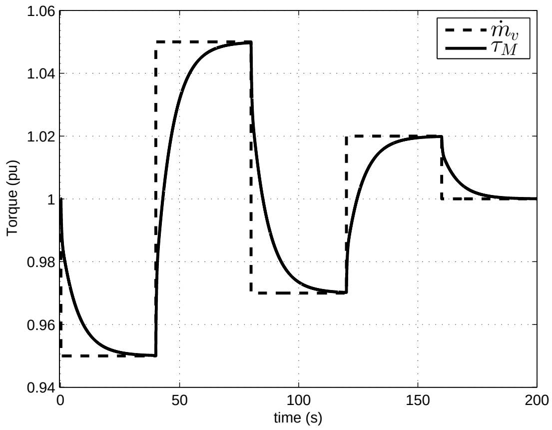

Figure 4: Random input simulation.

Table 1: Simulation parameters (Kundur *et al.*, 1994).

T_{ch}	0.3 s	k_{hp}	0.3
T_{re}	7 s	k_{ip}	0.3
T_{cr}	0.5 s	k_{lp}	0.4

3.1 Particle Swarm Optimization

Particle Swarm Optimization (PSO) is a stochastic optimization technique first presented by Kennedy and Eberhart (1995). The algorithm is based on the behaviour of bird flocking and fish schooling. The main PSO idea is similar to other evolutionary computation techniques such as Genetic Algorithms (GA).

Since its begin, the application of PSO has increased in many fields beyond engineering, such as psychology (Kennedy, 1997), product design (Yildiz, 2009) and economy (Moraes and Nagano, 2012).

The increase on PSO related research are justified due to its faster and cheaper convergence compared to other methods when applied to nonlinear systems, besides having only few adjustment parameters (Valdez and Melin, 2007).

The concept of the optimization consists of updating the particle position and speed towards its best solution. Each particle is updated using its own best found position and the global swarm best position, which makes the convergence to the final solution faster. It is easily demonstrated by the following equations, which correspond to the *canonical* PSO introduced by Clerc and Kennedy (2002):

$$\boldsymbol{v}_i^{t+1} = \chi\left[\boldsymbol{v}_i^t + \varphi_1 \boldsymbol{U}_1(0,1) * \left(\boldsymbol{p}_i - \boldsymbol{x}_i^t\right) + \varphi_2 \boldsymbol{U}_2(0,1) * \left(\boldsymbol{s} - \boldsymbol{x}_i^t\right)\right] \tag{26}$$

$$\boldsymbol{x}_i^{t+1} = \boldsymbol{x}_i^t + \boldsymbol{v}_i^{t+1} \tag{27}$$

being the *constriction factor* χ given by,

$$\chi = \frac{2k}{\left|2 - \varphi - \sqrt{\varphi^2 - 4\varphi}\right|} \tag{28}$$

where $\boldsymbol{v}_i^t$ and $\boldsymbol{x}_i^t$ are the speed and position of the particle i, respectively, $\boldsymbol{p}_i$ is the own best particle solution, $\boldsymbol{s}$ is the best swarm solution, φ_1 and φ_2 are constants called *cognitive* and *social* acceleration coefficients, $\boldsymbol{U}_1(0,1)$ and $\boldsymbol{U}_2(0,1)$ are random values $\in [0,1]$, $*$ is an element-by-element vector multiplication operator, k is an arbitrary coefficient usually set to 1 and $\varphi = \varphi_1 + \varphi_2$, being usually $\varphi_1 = \varphi_2 = 2.05$ (Eberhart and Shi, 2000).

Therefore, utilizing Eq. 25 in the algorithm represented by equations 26 and 27, the identified parameters of turbine's linearized model are shown in Tab. 2.

Table 2: Identified parameters from the linearized model (Eq. 25).

K_1	-4.5967	K_7	0.0184	K_{13}	-5.8051e^{-6}	K_{19}	-5.3031e^{-5}	K_{25}	3.3594e^{-5}
K_2	-3.463e^4	K_8	1.3309e^3	K_{14}	-0.2137	K_{20}	2.701	K_{26}	-0.1972
K_3	8.6601e^4	K_9	-0.2739	K_{15}	0.5644	K_{21}	-2.8904e^{-4}	K_{27}	1.9066e^{-4}
K_4	-8.8207e^{-5}	K_{10}	-1.6579e^3	K_{16}	8.5759e^3	K_{22}	-3.3701	K_{28}	-0.4209
K_5	-3.7704	K_{11}	-4.8719e^{-6}	K_{17}	-3.516	K_{23}	1.7491e^{-5}		
K_6	1.4502	K_{12}	0.2205	K_{18}	-7.3712e^3	K_{24}	-0.1133		

3.2 Internal Parameters Determination

While some parameters of the nonlinear model depicted in Fig. 3 are known in advance, some others can only be determined utilizing the results obtained by the PSO algorithm, which are shown in Tab. 2. As state previously, the calculations for obtaining constants K_1-K_{28} are omitted in this paper for better readability. However, making use of them along with the previously known constants and the identified ones, one is able to build a system with n equations owing n unknown parameters, becoming possible the solution through ordinary mathematical techniques.

Nevertheless, four further assumptions must be done in order to proceed with system's internal parameter estimation:

- the *Reheater* is assumed to be cylindrical, *i.e.* its surface area is given by $A_q = 2\sqrt{\pi l V_{re}}$, where $l > 0$ is the length of the vessel and, in this case, it can be arbitrarily chosen.
- the friction coefficient $k_f(\dot{m})$ must be a nonlinear function due to its dependence on the flow. One should notice that in Fluid Mechanics the friction increases geometrically with regarding to the flow. Therefore, through empiric numerical simulations for testing its behavior, the friction coefficient is assumed to be $k_f(\dot{m}) = k_f\dot{m}^2 + 370k_f\dot{m}$;
- the mixture of dry air into steam is assumed to be 10%;
- the room temperature of the *Reheater* is assumed to be the temperature of the heating element, which in this case is considered $0.7 \cdot T_u$.

Using the cited assumptions and the previous known constants (detailed in Tab. 3), the identified parameters of the nonlinear model are summarized in Tab. 4.

Table 3: System constants

γ	1.337 [1]	R	444.06 [J/kg/K]
T_u	903 [K]	l	10 [m]
P_0	1e^5 [Pa]	T_0	293 [K]
$\dot{m}_0$	735 [kg/s]	k_{hp}	0.3 [1]
k_{ip}	0.3 [1]	k_{lp}	0.4 [1]

Table 4: Identified parameters

V_{ch}	6.3 [m^3]	A_{ch}	0.052 [m^2]
V_{re}	190.5 [m^3]	A_{re}	0.116 [m^2]
V_{cr}	29.6 [m^3]	A_{cr}	0.26 [m^2]
$k_{f_{hp}}$	274.37 [(kg K m^2)$^{-1}$]	λ_0	260.14 [W/K/m^2]
$k_{f_{ip}}$	47.67 [(kg K m^2)$^{-1}$]	$k_{f_{lp}}$	6.3 [(kg K m^2)$^{-1}$]

It is important to highlight that the friction coefficient of the Low Pressure section $k_{f_{lp}}$ is not directly identified in this approach due to its cancellation during the linearization step. Therefore this constant must be set empirically through simulations.

3.3 Evaluation of the proposed model

The full system is evaluated in Matlab/Simulink® using Runge-Kutta 4$^{\text{th}}$-order solver with a time step of $t_s = 1$ ms. The three steam turbine models presented in this paper are evaluated: simplified (Fig. 2), nonlinear (Fig. 3) and linearized

(Eq. 25). Figure 5 shows the comparison between the models, whereas Tab. 5 presents the obtained fitting percentage for the shown time frame taking the results of the simplified model as reference and utilizing the coefficient of determination presented in Eq. 29, being y, $\hat{y}$ and $\overline{y}$ the measured, the estimated and the mean value of the measured output, respectively.

From the obtained results it is clear that the behaviors of the proposed models are close to the presented by the simplified one. In other words it means that, if the simplified model is widely used in literature and the proposed nonlinear one and its linearization are also able to depict the behavior of a steam turbine properly, one can conclude that both proposed model could also be used whenever the aim is power systems stability analysis.

However, the major advantage of the models proposed in this paper is that they allow the access to turbine's internal states, namely P_{ch}, P_{re}, P_{cr}, T_{ch}, T_{re}, T_{cr}. As mentioned in Sec. 1 and shown in the following ones, this special feature gives more possibilities whenever one aims the control of the steam turbine.

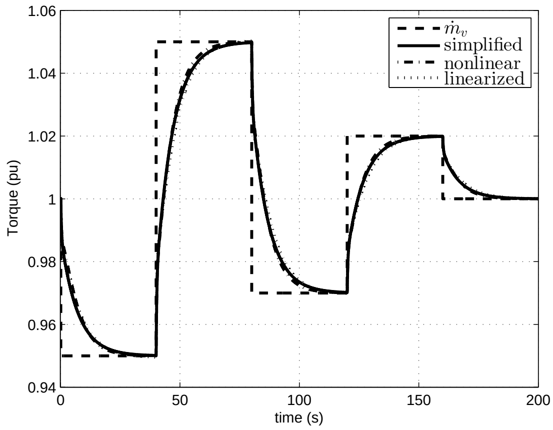

Figure 5: Comparison between models.

Table 5: Fitting percentage of proposed models.

Model	Fit %
Nonlinear	97.13
Linearized	96.10

$$\text{fit} = 100 \cdot \left(1 - \frac{||y - \hat{y}||}{||y - \overline{y}||}\right) \tag{29}$$

4. CLOSED-LOOP SYSTEM

The idea of having access to the internal states of a model leads immediately to the design of a state feedback for controlling system's output. However, in the present case of the steam turbine proposed model the states are not accessible through measurement, which leads one also to the design of a state observer. This section addresses exactly these two issues, namely the observer and controller design, besides of presenting also the usual approach for controlling turbine's speed.

It is important to highlight that the system to be controlled is not merely the steam turbine. The main idea behind the closed-loop system is to attach the turbine to the generator and consider the new system as a whole. It allows the measurement of generator's active power P_E, which is almost equivalent to its electrical torque τ_E. Since mechanical and electrical torques must be equal for the system to keep its steady condition, P_E is the natural variable to be fed back aiming the control of the whole system. Therefore the controller is called *power controller*.

The complete system is comprised by valve, turbine, generator, active power sensor, power controller, exciter and Automatic Voltage Regulator (AVR). The last two control generator's terminal voltage u_t and will not be analyzed in this paper. For simplicity, the valve is considered as a first-order linear system with unitary gain and time constant $\mathrm{T}_v = 0.4$ s. Equation 25 is implemented for the turbine, whereas generator's model is regarded according Kundur *et al.* (1994). Figure 6 shows the closed-loop system with its main blocks.

The system under consideration is meant to be a Single Machine Infinite Bus (SMIB), *i.e.* the frequency and voltage from the grid are constant and rated and they are not influenced by the plant. Besides, the active power sensor introduces some amount of white noise and quantization in the feedback system due to its intrinsic characteristics. In the present case, the variance of measurement noise is $\sigma^2 = 0.01$ and the quantization time is $t_s = 70$ ms.

Controller Design

Due to sensor's quantization, controllers designed in this section are regarded on its digital form, *i.e.* the sampling time is taken into account when designing and implementing them.

Two different controllers are experimented: a Proportional-Integral (PI) and the so called Linear Quadratic Gaussian (LQG). The former is based on VDI/VDE (2000) and is meant to be the most used one in practical implementations due to its easy tuning and understanding of the whole process. The latter is a state space controller which uses a cost function to be minimized in order to obtain its gains, besides utilizing the noise information on its design aiming the minimization of controlled output and control signal variances. For both controllers it is also implemented a feedforward strategy connected to the reference P_{ref} and with gain $K_f = 0.8$ in order to ensure faster convergence to the set-point. This strategy is common use according to literature, see *e.g.* VDI/VDE (2000).

Important to highlight is the fact that this paper does not intend to present an optimum tuning for the presented controllers, but rather comparing the common approach (PI) to an alternative one (LQG) in order to show advantages and drawbacks on their designs and main simulation results. For this reason the way of tuning the controllers will not be exploited in details.

VDI/VDE simplified controller VDI/VDE (2000) shows a simple control structure to be used on generating units. It is represented by a Proportional (P) and a Proportional-Integral (PI) controllers, where the first controls rotor's speed and the latter controls the active power. In fact, the speed controller is seldom used in rated operation, since its main aim is the speed control during the start-up of the unit or island configuration. Therefore only the active power PI controller is utilized in this work. Its gains are set heuristically according to system's output response. In this case it was chosen $K_p = 0.2$ and $T_n = 10$ s.

Linear Quadratic Gaussian The Linear Quadratic Gaussian controller, shortly LQG, is regarded as the most fundamental optimal controller, making use of a Kalman Filter (KF) and a Linear Quadratic Regulator (LGR), therefore the approach is meant as a state space control. Its main features are state observation and the way of noise treatment due to the KF, and the use of two weighting matrices (Q and R) which are responsible for determining output's behavior. Due to the Separation Theorem, KF and LQR can be set independently.

In the most usual way LQG is tuned using the value of noise's variance σ^2 and state disturbance vector Υ, where the latter is identified setting systems' input to null and applying only the noise signal to it. The identified state disturbance vector is,

$$\Upsilon = \left[\begin{array}{cccccc} 9.724 & 2.06 & 1.51 & 7.53 & -1.323 & 1.523 \end{array}\right]^T \cdot 10^{-4}. \tag{30}$$

Being the main purpose of controller's design reference tracking and noise/disturbance rejection, the system is augmented in one order to ensure null error in steady state for step references/disturbances (Ogata, 1970), *i.e.* all original matrices and vectors presented in Eq. 25 are augmented in one order, as well as vector Υ. System's controllability and observability are both ensured with this approach.

Controller's tuning free parameter is the 7^{th} entry of the augmented vector Υ, named here υ_t. LQR's matrices are set to $Q = \Upsilon_a \sigma^2 \Upsilon_a^T$ and $R = \sigma^2$. It is important to highlight that this control approach is only possible due to system's state space representation (Eq. 25) and unknown parameter determination (Tab. 2).

In next section both presented control approaches are evaluated and the results of output's closed-loop system are compared.

5. EVALUATION

For evaluation of the closed-loop system, two different simulations are defined: noise and disturbance rejection; and set-point tracking.

The former is simulated by considering the previous cited white noise to the active power sensor, a short circuit at grid voltage and a torque disturbance. The short circuit lasts 200 ms and starts at $t = 5$ s. Torque disturbance decreases turbine's output torque level in 25%, lasts 5 s and starts at $t = 25$ s. Figure 7 shows the mechanical torque τ_M, the frequency ω_r and the control signal u for both presented controllers.

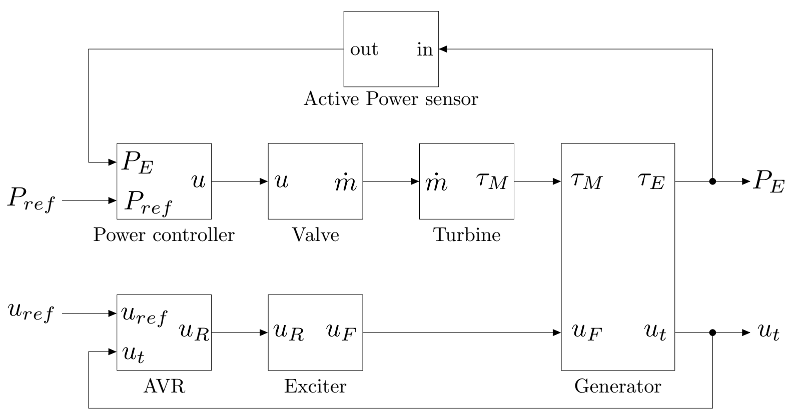

Figure 6: Closed-loop system.

Worth noticing is that unit's frequency ω_r for both controllers are equal. In fact, for a fair comparison, this result is obtained through the tuning of LQG's free parameter υ_t until frequency's variance σ_f^2 for LQG matches the one for PI controller. In this case, $\sigma_f^2 = 1.7e^{-5}$ for both controllers, while the variances of control signals are $\sigma_{\text{PI}}^2 = 3.7e^{-3}$ and $\sigma_{\text{LQG}}^2 = 6.7e^{-4}$. Besides, LQG's control signal does not reach its upper limit, while PI's does. Further, the mechanical torque presents less oscillations when using LQG, also due to the smaller variance of its control signal.

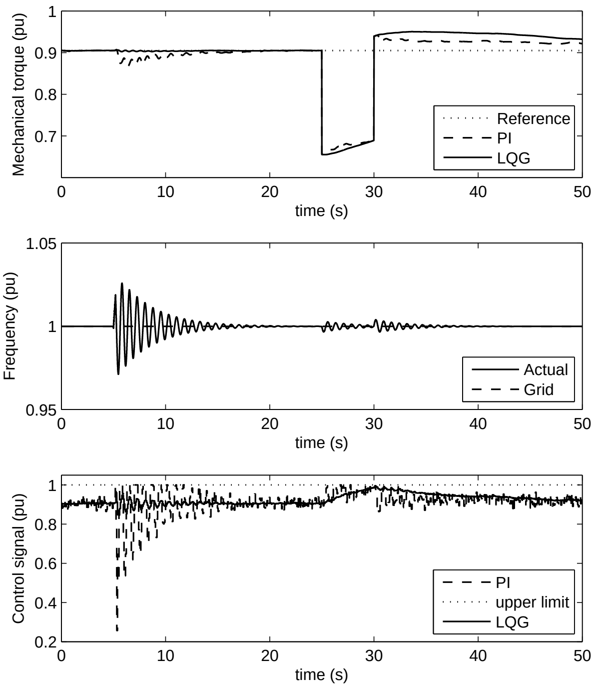

Figure 7: Noise and disturbance evaluation.

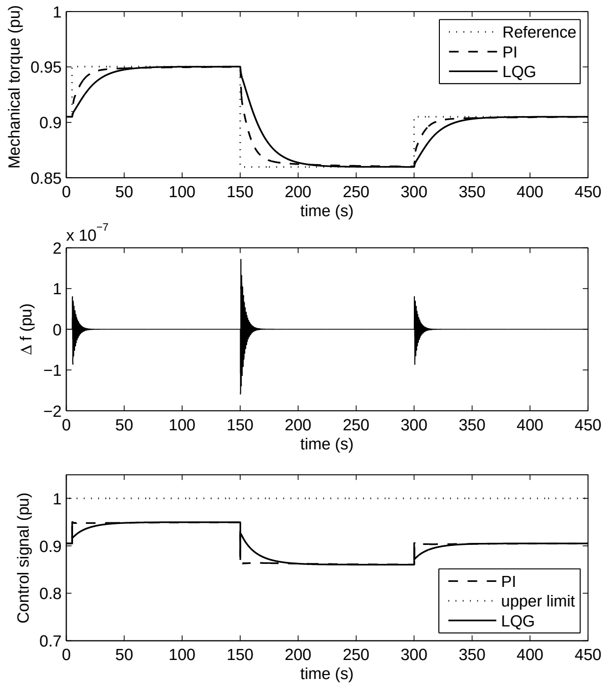

Figure 8: Reference tracking evaluation.

For the case of reference tracking simulation, noise and disturbances are neglected. The active power set-point is changed to $\pm 5\%$ from its rated value. Figure 8 presents the results for the electrical torque τ_E, frequency variation Δf and control signal u. In regard to the figure, it is possible to notice that the frequency has no relevant change. This is due to turbine's slow dynamics, which allows the electrical torque to match mechanical one. Also, the system simulated with LQG controller takes longer – roughly 10 s more – to reach the reference than one with PI.

6. CONCLUSIONS

This paper has shown an innovative state space approach for the modelling of steam turbines aiming on its parameter identification and further optimal control.

The identification results, carried out using a PSO algorithm, has shown that both presented nonlinear and linearized models are able to depict system's dynamics with accuracy of more than 96% with the widely used simplified model as basis. This result proves that, with aim in power system stability analysis, any of the three models depicted in this paper can be used in simulation of generating units.

Nevertheless, it is clear that nonlinear and linearized models give more alternatives whenever one deals with controller design, since both are state space approaches, *i.e.* one has access to turbine's internal states, as P_{ch}, P_{re}, P_{cr}, T_{ch}, T_{re} and T_{cr}, apart from torque's output τ_M.

This result has led to the design of LQG, an optimal controller consisted by a state observer (KF) and state feedback (LQR) which considers on its design the stochastic part of the process, *i.e.* the measurement noise. In comparison to an ordinary PI controller, LQG results are quite interesting.

For instance, despite of reference tracking being more effective with PI, the LQG result could also be considered acceptable for practical purposes. However, perhaps the most interesting result for the proposed closed-loop system is its noise rejection. Control signal variance is 5.5 times smaller for LQG than for PI controller considering the same frequency variance $\sigma_{\omega_r}^2$. When one thinks that the control signal shown in Fig. 7 will be applied to a mechanical device, *i.e.* the control valve, it is clear that its variance reduction is mandatory aiming longer device's working hours, besides giving better results, with less oscillations in active power control.

Next steps on this research will consider real turbine data to be used in the identification process, in addition to other control approaches, such as predictive, adaptive and robust.

7. ACKNOWLEDGEMENTS

R. Trentini acknowledges the financial support of the Brazilian Research Agency (CNPq).

8. REFERENCES

Ali, H.I., Bahari, S., Noor, B.M., Bashi, S.M. and Marhaban, M.H., 2009. "A review of pneumatic actuators (Modeling and Control)". *Australian Journal of Basic and Applied Sciences*, Vol. 3, No. 2, pp. 440–454.

Blagojević, V. and Stojiljković, M., 2007. "Mathematical and Simulink model of the pneumatic system with bridging of the dual action cylinder chambers". *Facta Universitatis — Mechanical Engineering*, Vol. 5, No. 1, pp. 23–31.

Bobrow, J.E. and McDonell, B.W., 1998. "Modeling, identification, and control of a pneumatically actuated, force controllable robot". *IEEE Transactions on Robotics and Automation*, Vol. 14, No. 5, pp. 732 –742.

Brun, X., 1999. *Commandes linéaires et non linéaires en électropneumatique. Méthodologies et Applications.* Ph.D. thesis, Institut national des sciences appliquées de Lyon (INSAL).

Carneiro, J.F. and Almeida, F.G., 2006. "Reduced-order thermodynamic models for servo-pneumatic actuator chambers". In *Proceedings of the Institution of Mechanical Engineers, Part I: Journal of Systems and Control Engineering*. Vol. 220, pp. 301–314.

Chaibakhsh, A. and Ghaffari, A., 2008. "Steam turbine model". *Simulation Modelling Practice and Theory*, Vol. 16, No. 9, pp. 1145 – 1162.

Clerc, M. and Kennedy, J., 2002. "The particle swarm - explosion, stability, and convergence in a multidimensional complex space". *IEEE Transactions on Evolutionary Computation*, Vol. 6, pp. 58 – 73.

Eberhart, R. and Shi, Y., 2000. "Comparing inertia weights and constriction factors in particle swarm optimization". In *Proceedings of the 2000 IEEE Congress on Evolutionary Computation*. IEEE Press, Piscataway, USA, pp. 84 – 88.

Eremia, M. and Shahidehpour, M., 2013. *Handbook of Electrical Power System Dynamics: Modeling, Stability, and Control*. IEEE Press Series on Power Engineering. Wiley.

Fox, R.W. and McDonald, A.T., 2008. *Introduction to Fluid Mechanics*. Wiley.

Grainger, J.J. and Stevenson, W.D., 1994. *Power system analysis*, Vol. 621. McGraw-Hill New York.

Grigsby, L., 2012. *Power System Stability and Control, Third Edition*. The electric power engineering handbook. CRC Press.

Jiang, P., Gao, L. and Dai, Y., 2010. "A new non-linear model of steam turbine unit for dynamic analysis of power system". In *Power System Technology (POWERCON), 2010 International Conference on*. pp. 1–6.

Kennedy, J., 1997. "The particle swarm: social adaptation of knowledge". In *Evolutionary Computation, 1997., IEEE International Conference on*. pp. 303–308.

Kennedy, J. and Eberhart, R., 1995. "Particle swarm optimization". In *Proceedings of IEEE International Conference on Neural Networks*. IEEE Press, Piscataway, USA, pp. 1942 – 1948.

Kundur, P., Balu, N.J. and Lauby, M.G., 1994. *Power system stability and control*, Vol. 7. McGraw-Hill New York.

Moraes, M.B.C. and Nagano, M.S., 2012. "Cash balance management: A comparison between genetic algorithms and particle swarm optimization". *Acta Scientiarum. Technology*, Vol. 34, No. 4, pp. 373 – 379.

Ogata, K., 1970. *Modern control engineering*. Prentice-Hall electrical engineering series. Prentice-Hall.

Richer, E. and Hurmuzlu, Y., 2000. "A High Performance Pneumatic Force Actuator System Part 1 - Nonlinear Mathematical Model". *ASME Journal Dynamic Systems: Measurement and Control*, Vol. 122, No. 3, pp. 416–425.

Valdez, F. and Melin, P., 2007. "Parallel evolutionary computing using a cluster for mathematical function optimization". In *Fuzzy Information Processing Society, 2007. NAFIPS '07. Annual Meeting of the North American*. pp. 598–603.

VDI/VDE, 2000. "Guidelines for testing control systems of steam turbines - Dynamic behavior of speed and load control - VDI/VDE 3521".

Yildiz, A.R., 2009. "A novel particle swarm optimization approach for product design and manufacturing". *The International Journal of Advanced Manufacturing Technology*, Vol. 40, pp. 617 – 628.

Zimmer, G., 2008. "Modelling and simulation of steam turbine processes: individual models for individual tasks". *Mathematical and Computer Modelling of Dynamical Systems*, Vol. 14, No. 6, pp. 469–493.

9. RESPONSIBILITY NOTICE

The authors are the only responsible for the printed material included in this paper.